# Zebrafish type I collagen mutants faithfully recapitulate human type I collagenopathies

Charlotte Gistelinck[a,b], Ronald Y. Kwon[b], Fransiska Malfait[a], Sofie Symoens[a], Matthew P. Harris[c,d], Katrin Henke[c,d], Michael B. Hawkins[c,d], Shannon Fisher[e], Patrick Sips[a], Brecht Guillemyn[a], Jan Willem Bek[a], Petra Vermassen[a], Hanna De Saffel[a], Paul Eckhard Witten[f], MaryAnn Weis[b], Anne De Paepe[a], David R. Eyre[b], Andy Willaert[a,1,2], and Paul J. Coucke[a,1]

[a]Center for Medical Genetics Ghent, Ghent University, 9000 Ghent, Belgium; [b]Department of Orthopaedics and Sports Medicine, University of Washington, Seattle, WA 98195; [c]Department of Genetics, Harvard Medical School, Boston, MA 02115; [d]Department of Orthopaedic Research, Boston Children's Hospital, Boston, MA 02115; [e]Department of Pharmacology & Experimental Therapeutics, Boston University School of Medicine, Boston, MA 02115; and [f]Biology Department, Research Group Evolutionary Developmental Biology, Ghent University, 9000 Ghent, Belgium

The type I collagenopathies are a group of heterogeneous connective tissue disorders, that are caused by mutations in the genes encoding type I collagen and include specific forms of osteogenesis imperfecta (OI) and the Ehlers–Danlos syndrome (EDS). These disorders present with a broad disease spectrum and large clinical variability of which the underlying genetic basis is still poorly understood. In this study, we systematically analyzed skeletal phenotypes in a large set of zebrafish, with diverse mutations in the genes encoding type I collagen, representing different genetic forms of human OI, and a zebrafish model resembling human EDS, which harbors a number of soft connective tissues defects, typical of EDS. Furthermore, we provide insight into how zebrafish and human type I collagen are compositionally and functionally related, which is relevant in the interpretation of human type I collagen-related disease models. Our studies reveal a high degree of intergenotype variability in phenotypic expressivity that closely correlates with associated OI severity. Furthermore, we demonstrate the potential for select mutations to give rise to phenotypic variability, mirroring the clinical variability associated with human disease pathology. Therefore, our work suggests the future potential for zebrafish to aid in identifying unknown genetic modifiers and mechanisms underlying the phenotypic variability in OI and related disorders. This will improve diagnostic strategies and enable the discovery of new targetable pathways for pharmacological intervention.

skeletal phenomics | type I collagen | type I collagenopathies | zebrafish models | osteogenesis imperfecta

Collagens are a large family of diverse, structural extracellular matrix proteins, among which fibril-forming molecules dominate. Type I collagen is the most abundant fibrillar collagen in vertebrates, encoded by two genes, the COL1A1 and the COL1A2 genes that express the α1(I) and α2(I) chain, respectively. In the endoplasmic reticulum, after extensive posttranslational modification of proline and lysine residues, two associated proα1(I) chains and one proα2(I) chain fold into a left-handed triple-helical linear molecule. The characteristic repetitive Gly-X-Y triplet sequence of the helical domain (X frequently proline, and Y frequently hydroxyproline) produces a tightly intertwined trimeric conformation (1). During the secretion of the native procollagen molecules into the structural extracellular matrix and assembly into fibrils, first the carboxypropeptides and then the amino-propeptides are removed by propeptidases.

Genetic mutations in the type I collagen-encoding genes are associated with a group of rare and heterogeneous disorders, the type I collagenopathies, which encompass specific forms of osteogenesis imperfecta (OI), the Ehlers–Danlos syndrome (EDS), and Caffey disease (2). Caffey disease, or infantile cortical hyperostosis, is a rare condition caused by a specific Arg to Cys substitution (p.R836C) in the α1(I) chain of type I collagen and is characterized by an inflammatory process with swelling of soft tissues and periosteal hyperostosis of some bones (2). OI, which is a disorder characterized by a low bone mass and a high bone fragility in human patients, is predominantly caused by dominant mutations in COL1A1 or COL1A2 (3). According to the original classification by Sillence et al. (4), these COL1A mutations underlie the classic subtypes of OI (types I–IV), which at a biochemical level are effected by either quantitative or qualitative defects in type I collagen fibrils. OI type I, the mildest form of the disease, generally arises due to mutations that cause a premature stop codon in COL1A1, creating a functional null allele, so that only half of the normal amount of type I collagen is synthesized (5). The presence of one COL1A2-null allele is not associated with a disorder, while a complete loss of COL1A2 causes the cardiac valvular subtype of EDS, which is associated with variable joint hypermobility and skin fragility, and early-onset severe cardiac valvular problems, rather than bone fragility (6). In the more severe phenotypes of classic OI (OI types II, III, and IV), type I collagen exhibits a structural defect. The great majority of causative mutations in these types are single nucleotide changes, giving rise to the substitution of a Glycine

## Significance

Type I collagenopathies are a heterogenous group of connective tissue disorders, caused by genetic defects in type I collagen. Inherent to these disorders is a large clinical variability, of which the underlying molecular basis remains undefined. By systematically analyzing skeletal phenotypes in a large set of type I collagen zebrafish mutants, we show that zebrafish models are able to both genocopy and phenocopy different forms of human type I collagenopathies, arguing for a similar pathogenetic basis. This study illustrates the future potential of zebrafish as a tool to further dissect the molecular basis of phenotypic variability in human type I collagenopathies, to improve diagnostic strategies as well as promote the discovery of new targetable pathways for pharmacological intervention of these disorders.

residue for a bulky, polar, or charged amino acid, disrupting the highly conserved Gly-X-Y triplet sequence. Following the Sillence et al. (4) classification, type IV is described as being moderate, type III as severe or progressively deforming, and type II as causing perinatal lethality. Besides the classic types of OI, mutations in noncollagenous genes have been reported to mostly cause autosomal recessive forms of OI. These genes generally encode for proteins that interact with type I collagen, acting as key players in processes such as collagen synthesis, collagen folding and posttranslational modification, intracellular trafficking of collagen, or collagen fibril cross-linking (5).

Inherent to the pathology of OI is a large clinical variability, with phenotypes ranging from nearly asymptomatic with a mild predisposition to fractures and a normal lifespan, to forms associated with multiple fractures and severe deformities already present in utero that may cause perinatal lethality (7). In the classic dominant forms of OI types II–IV, some general principles have emerged for genotype–phenotype correlations (3, 8). Mutations in *COL1A1* are generally associated with a more severe phenotype than mutations in *COL1A2*. Furthermore, the position of mutations along the α-chains can modulate the outcome. Nevertheless, numerous exceptions to these guidelines have already been demonstrated (9). Of note, extensive phenotypic variability resulting from identical mutations has been described in recent years to be common in both dominant and recessive forms of OI (10–12). This renders prediction on the clinical outcome of certain mutations in OI particularly challenging. Dissecting the underlying basis of this phenotypic variability is crucial to enable a more profound understanding of molecular mechanisms in OI, to enable the discovery of new targetable pathways for intervention, and to identify novel biomarkers for diagnostics and monitoring of pharmacological treatments.

To study human skeletal dysplasias, zebrafish (*Danio rerio*) models are increasingly being used as a valuable complementation or predecessors to the traditional murine models (13, 14). Besides their unique attributes, such as the rapid development, large offspring numbers, and ease and speed in generating mutant lines, zebrafish bone mutants tend to survive into adulthood far more easily than corresponding mouse models, making them also available for the study of later stages of skeletal development and maturation (13, 15). Furthermore, due to the high conservation of developmental programs in osteogenesis between teleosts and mammals, functional gene and pathway analysis in zebrafish can yield relevant insights into human bone disease (16). Detailed reports have already documented similarities and differences between teleost and mammalian bone biology that are relevant for modeling human bone disease (13, 14, 17, 18). One of these differences is the composition of type I collagen in zebrafish, which harbors not one but two orthologs of the human *COL1A1* gene, namely *col1a1a* and *col1a1b*, encoding the α1- and α3-chain, respectively. Although some characteristics of zebrafish type I collagen have already been addressed (19), more insight into the functional implications of this additional teleost-specific α-chain is needed.

In recent years, different zebrafish mutants have already been reported to accurately model certain genetic types of human OI (20–23). However, these studies were focused on a detailed analysis of single mutants, modeling certain subtypes of OI, while the greatest strength of the zebrafish lies in the ease of accommodating the parallel analysis of multiple mutant models. Moreover, recent advances in μCT-based methods enable detailed and rapid skeletal phenotyping of zebrafish mutants, which often have been resistant to such methodologies (24). Advances in processing and analysis have now allowed analysis of hundreds of morphological and densitometric traits in large sets of zebrafish skeletal mutants (25). In this work, we applied systematic collagen analysis with skeletal phenomics to characterize a large set of zebrafish with mutations in type I collagen genes, as

seen in patients with different forms of classical OI and EDS, to assess to which extent key features of human type I collagenopathies are recapitulated.

## Results

### Zebrafish with Different Mutations in Type I Collagen Show Variable Skeletal Phenotypes.
We systematically analyzed skeletal phenotypes in a large set of zebrafish models carrying different mutations in the zebrafish type I collagen-encoding genes *col1a1a*, *col1a1b*, and *col1a2* (Table 1). As a reference, we also included two knockout mutants, $bmp1a^{-/-}$ and $plod2^{-/-}$, representing severe recessive forms of OI with defects in type I collagen processing and cross-linking, respectively (22). Upon μCT scanning, we observed a large diversity of skeletal phenotypes throughout the whole set of mutants. Severe morphological abnormalities included callus formation, bowing and kinking of the ribs, malformation of the vertebral column, short stature, and craniofacial abnormalities (Fig. 1, Table 2, and *SI Appendix*, Fig. S1), indicating compromised bone quality. Next, we performed μCT-based phenomic profiling (25) (*SI Appendix*, Fig. S2) to quantify 200 different descriptors of bone morphology and mineralization in the axial skeleton of each animal. Specifically, we segmented each of 20 vertebrae into three skeletal elements—the neural arch (Neur), centrum (Cent), and haemal arch/ribs (Haem)—and for each skeletal element, we computed four primary parameters: tissue mineral density (TMD, mgHA/cm3), volume (Vol, μm$^3$), and thickness (Th, μm), and also centrum length (Cent.Le, μm). In total, we analyzed 28,000 phenotypic data points derived from 140 different animals. To explore intergenotype variability for each trait, means were calculated within each genotype (mutant and control) and normalized to the SD of their respective control population [z-score = (mean value mutant − mean value control)/SD control]. In general, we observed a large diversity of skeletal phenotypes throughout the whole set of mutants (Fig. 2). We found that phenotypic severity (as measured by the absolute value of the z-score) tended to be highest for mutants associated with collagen processing (*plod2*, *bmp1a*) and qualitative collagen defects (e.g., $col1a1a^{chi/+}$, $col1a2^{dmh15/+}$, $col1a1b^{dm29/+}$), and lower for mutants associated with quantitative collagen defects (e.g., $col1a1a^{+/-}$, $col1a1b^{-/-}$, $col1a2^{-/-}$). Remarkably, some mutants with qualitative defects (and collagen processing defects) exhibited a pronounced enrichment of positive z-scores for some traits (e.g., Cent. TMD). We interpret the different degrees of phenotypic severity in mutants associated with qualitative or quantitative collagen defect, as well as the variability in direction of effect (i.e., positive or negative effect on bone mass or mineralization) across genotypes, to reflect the clinical variability observed in human type I collagenopathies.

### Heterozygous Loss of both α1(I) and α3(I) in Zebrafish Is Reminiscent of Mild OI Type I.
Human patients with a heterozygous *COL1A1*-null allele (*COL1A1* haploinsufficiency) develop OI type I, characterized by short or normal stature, mild bone fragility, relatively few fractures, and minimal limb deformities. In zebrafish two orthologs of the human *COL1A1* exist, namely *col1a1a* encoding α1(I) and *col1a1b* encoding α3(I). Two zebrafish knockout mutants with a premature stop-codon mutation in either *col1a1a* or *col1a1b* show absence of α1(I) and α3(I), respectively, in the vertebral bone (Fig. 3A and *SI Appendix*, Fig. S3). However, both qualitative and quantitative assessment of μCT scans of the vertebral column of heterozygous $col1a1a^{+/-}$ or $col1a1b^{+/-}$ zebrafish mutants revealed no skeletal abnormalities (Fig. 1 and *SI Appendix*, Figs. S4 and S5), which is most likely related to functional redundancy between both paralogs. Hence, we generated a double-heterozygous knockout mutant ($col1a1a^{+/-}$;$col1a1b^{+/-}$), which displays a mild skeletal phenotype, with a low frequency of spontaneous fractures (calluses

**Table 1. List of mutant zebrafish alleles analyzed in this study**

| Gene | Allele | Effect on protein level | Effect on homologous human protein |
|---|---|---|---|
| Type I collagen knockout alleles (quantitative defect) | | | |
| col1a1a | sa1748 | p.(Gly1179X) | |
| col1a1b | sa12931 | p.(Cys68X) | |
| col1a2 | sa17981 | p.(Ala154Cysfs*23) | |
| Type I collagen amino acid substitutions (qualitative defect) | | | |
| col1a1a | chihuahua (chi) | p.(Gly736Asp) | α1(I) p.(Gly574Asp) |
| col1a1a | microwaved (med) | p.(Glu888Lys) | α1(I) p.(Glu726Arg) |
| col1a1a | dmh13 | p.(Gly1093Arg) | α1(I) p.(Gly931Arg) |
| col1a1a | dmh14 | p.(Gly1144Glu) | α1(I) p.(Gly981Glu) |
| col1a1b | dmh29 | p.(Gly1123Asp) | α1(I) p.(Gly958Asp) |
| col1a2 | dmh15 | p.(Gly882Asp) | α2(I) p.(Gly802Asp) |
| Knockout alleles in genes involved in Type I collagen processing | | | |
| bmp1a | sa2416 | p.(Arg522X) | |
| plod2 | sa1768 | p.(Tyr679X) | |

Mutant alleles are listed, along with the effect of the mutation on protein level (p-notation). For alleles causing an amino acid substitution, the corresponding effect on the homologous human protein is listed in the p-notation (35).

in the ribs), scoliosis and localized compression, fusions, and mild malformation of the vertebral bodies in some of the mutant fish (Figs. 1 and 4A and Table 2). Quantitative measures of bone

in this mutant revealed localized reduction of centrum volume, length, and TMD (*SI Appendix*, Fig. S6). However, these results were not found to be statistically significant throughout the entire
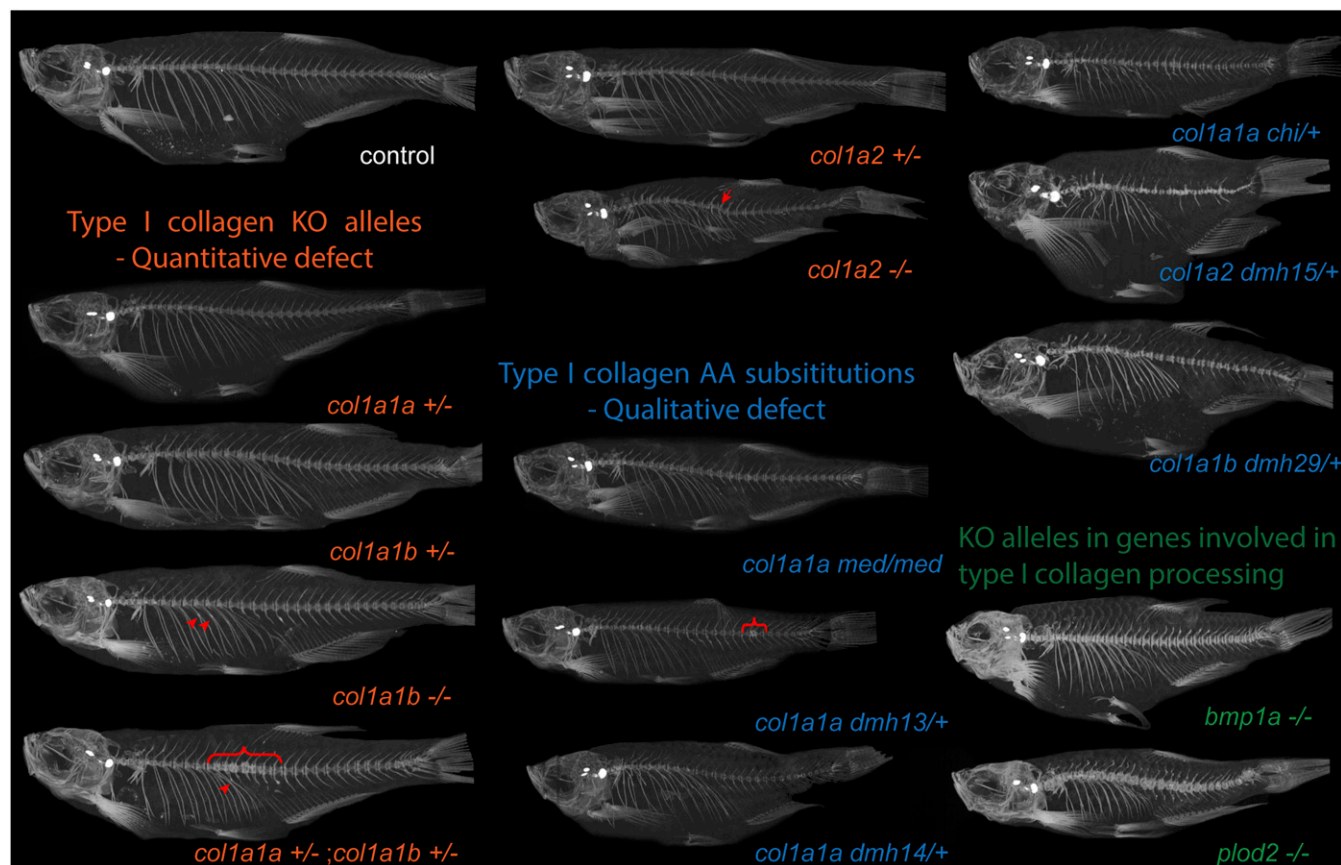


**Fig. 1.** μCT images of different zebrafish models with affected type I collagen. For μCT scanning, we included several mutants with a nonsense or splice mutation in *col1a1a*, *col1a1b*, or *col1a2*, generating a knockout of these genes (*col1a1a*$^{-/-}$ not viable). These mutants are grouped together and indicated as "type I collagen knockout (KO) alleles—quantitative defect" (shown in orange). Another set of mutants carries mutations resulting in substitutions [indicated as "type I collagen amino acid (AA) substitutions—qualitative defect, shown in blue] of a Gly residue in α1(I) (*col1a1a*$^{dmh13/+}$, *col1a1a*$^{dmh14/+}$ and *col1a1a*$^{chi/+}$), α2(I) (*col1a2*$^{dmh15/+}$), or α3(I) (*col1a1b*$^{dmh29/+}$). The microwaved (*col1a1a*$^{med/med}$) mutant carries a homozygous Glu substitution in α1(I). Finally, we included two mutant models with a knockout mutation in the *bmp1a* and *plod2* genes ("KO alleles in genes involved in type I collagen processing," shown in green). Representative fish from each mutant genotype are shown. Callus formation in ribs (arrowheads), local compressions of the vertebral column (brackets), and kyphosis (arrow), are indicated (also listed in Table 2).

MEDICAL SCIENCES

**Table 2. Phenotypical features observed upon μCT-scanning of adult mutant fish included in this study**

| Zebrafish mutant | Associated human disorder + unique clinical features | No. of animals with rib fracture callus | No. of animals with vertebral fusions | VC over/undermineralized (TMD, $P < 0.05$) | Kyphosis (K) and/or scoliosis (S) | Decreased bodylength–SL ($P < 0.0001$) |
|---|---|---|---|---|---|---|
| **Type I collagen knockout alleles (quantitative defect)** | | | | | | |
| col1a1a^{+/−} | OI type I, Mild. Normal | 0/5 | 0/5 | / | / | / |
| col1a1b^{+/−} | or short stature, little | 0/5 | 0/5 | / | / | / |
| col1a1a^{+/−};col1a1b^{+/−} | or no deformities | 1/5 | 2/5 | / | S | / |
| col1a1b^{−/−} | | 2/5 | 0/5 | / | / | / |
| col1a2^{+/−} | No disease | 0/5 | 0/5 | / | / | / |
| col1a2^{−/−} | EDS, cardiac valvular type | 0/5 | 0/5 | / | K | Y |
| **Type I collagen amino acid substitutions (qualitative defect)** | | | | | | |
| col1a1a[chi/+] | OI types II–IV, moderate | 5/5 | 5/5 | / | K + S | Y |
| col1a1a[med/med] | to severe/lethal. | 1/6 | 0/6 | Undermineralized | S | / |
| col1a1a[dmh13/+] | Short stature and | 1/6 | 4/6 | / | S | Y |
| col1a1a[dmh14/+] | bone deformities. | 0/5 | 1/5 | / | S | Y |
| col1a1b[dmh29/+] | Overmineralization | 5/6 | 6/6 | Overmineralized | K + S | Y |
| col1a2[dmh15/+] | (36) | 6/6 | 6/6 | Overmineralized | K + S | Y |
| **Knockout alleles in genes involved in type I collagen processing** | | | | | | |
| bmp1a^{−/−} | OI type XIII, severe. Marked overmineralization | 0/5 | 0/5 | Overmineralized | K + S | Y |
| plod2^{−/−} | Overlap BS–OI moderate/severe | 5/5 | 5/5 | Overmineralized | K + S | Y |

For each mutant model, the specific disorder and unique clinical features associated with a similar mutation in human patients is listed (7, 20). In addition, per genotype the ratio (no.) of animals that had at least one rib fracture callus (third column, never observed in any wild-type control animals), or fusion of vertebral bodies in the vertebral column (fourth column, only rarely detected in wild-type control animals) are given. TMD in the VC was quantified in FishCuT software and was indicated as "undermineralized" if significantly decreased or as "overmineralized" if significantly increased according to the global test ($P < 0.005$). The presence of kyphosis (K) or scoliosis (S) was also evaluated on 3D-scan images. Finally, the presence of a significant decrease ($P < 0.001$) in the mean body length, [i.e., the standard length (SL, measured from the tip of the snout to basis of the caudal fin) of mutant genotypes is indicated] (see *SI Appendix*, Fig. S20 for boxplots of SL measurements per genotype, compared with their wild-type siblings). Other abbreviations: BS, Bruck syndrome; VC, vertebral column.

length of the vertebral column, most likely due to the intragenotype phenotypic variability and incomplete penetrance, which is further demonstrated by the much larger spread of values for the different skeletal parameters in the group of mutant fish compared with control fish (Fig. 4B).

**A Complete Loss of Zebrafish α1(I), but Not α3(I), Causes Lethality in Early Larval Stages.** We next assessed the effect of a complete (homozygous) loss of α1(I) or α3(I) on survival and on skeletal integrity. In progeny resulting from an in-cross of col1a1a^{+/−}; col1a1b^{+/−} mutant fish, all possible genotypes were shown to be present at 7 d postfertilization (dpf), while from 15 dpf on some genotypes were underrepresented according to Mendelian predictions, or even lost (Fig. 5A). Eventually, all genotypes containing a homozygous knockout of col1a1a [loss of α1(I)] were found to be lethal by the age of 3 mo. Homozygous mutant col1a1b^{−/−} mutants [loss of α3(I)] were present by the age of 3 mo, however at reduced numbers if combined with heterozygous loss of col1a1a (col1a1a^{+/−};col1a1b^{−/−}). Fish with a complete loss of α3(I), but intact α1(I) did not show significant alterations of bone morphology (*SI Appendix*, Fig. S7), although some fish showed evidence of fractures (Fig. 1 and Table 2) and increased TMD throughout the vertebral column, indicating an impaired bone quality.

Because the knockout of col1a1a compromises viability from 7 dpf on, the general morphology of col1a1a^{−/−} mutant larvae was assessed at this stage. These larvae lacked the presence of an inflated swim bladder, a structure that is essential for survival once larvae are required to actively feed (Fig. 5B). Furthermore, the distal margins of the pectoral fins, and the finfold, were shown to be ruffled in these mutants (Fig. 5 B and C). These fin structures are structurally supported by fin actinotrichia, which are prefin-ray structures composed of collagen fibers (26). Upon detailed examination of the finfold, these actinotrichia were found to be absent in col1a1a^{−/−} mutant larvae (Fig. 5D). This is in concordance with earlier studies reporting these structures to only contain type I collagen as α1(I) homotrimers (26, 27), while in other tissues both α1(I) and α3(I) are present (26, 28).

**Complete Loss of α2(I) in Zebrafish Leads to Soft Connective Tissues Abnormalities, Reminiscent of the Human EDS.** We studied a zebrafish mutant with a splice mutation in col1a2, resulting in the absence of α2(I) (Fig. 3B). In humans, heterozygosity for COL1A2-null mutations (COL1A2 haploinsufficiency) is not known to be pathogenic, while a complete absence of α2(I) chains is associated with the cardiac valvular type of EDS, a connective tissue disorder characterized by skin fragility, joint hypermobility, early-onset, severe and progressive cardiac valvular defects, and mild osteopenia with increased risk of fractures in some patients (6, 29). Similarly, zebrafish with a heterozygous col1a2 knockout are asymptomatic (Fig. 6A and *SI Appendix*, Fig. S8), while homozygous col1a2 knockouts were severely affected with marked kyphosis of the vertebral column at the level of transitioning precaudal to caudal vertebrae (Figs. 1 and 6A, arrowhead). FishCuT analysis demonstrated a slightly lower mineralization in the vertebral column of col1a2^{−/−} mutant fish, although this was found not to be significant throughout the whole vertebral column (*SI Appendix*, Fig. S9). No rib fracture calluses were observed (Table 2). Histological analysis showed local alterations in bone thickness, fusions at some of the vertebral endplates, and loss of typical Sharpey fibers (Fig. 6D).
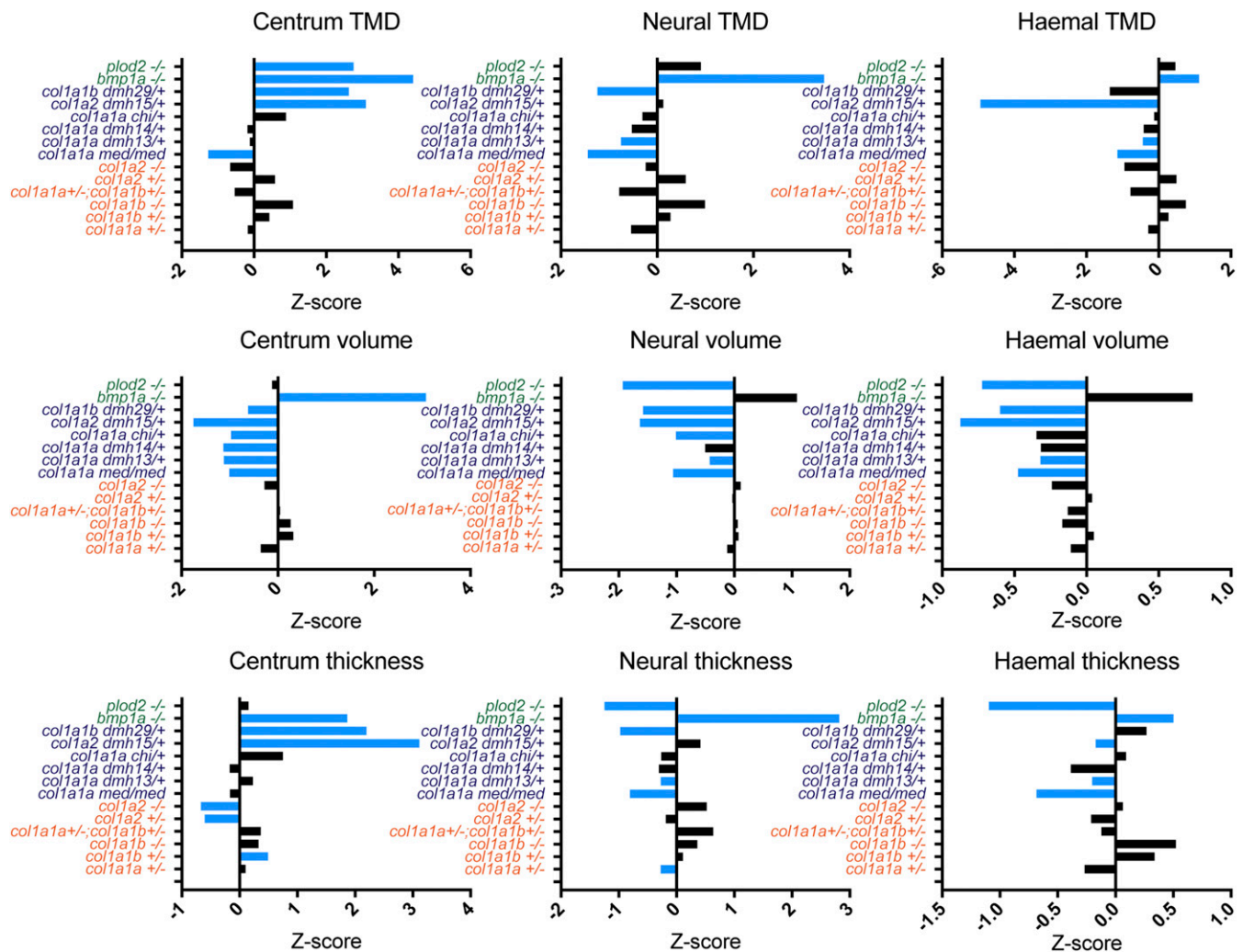
**Fig. 2.** Inter- and intragenotype phenotypic variability demonstrated by quantitative μCT analysis in FishCuT. For a set of parameters that quantify morphology and mineralization in the vertebral column of the different mutant populations, z-scores are given for each mutant genotype [z-score = (mean value mutant − mean value control)/SD control]. On the y axis, mutants associated with a collagen processing defect are indicated in green, mutants with a qualitative defect in type I collagen are indicated in dark blue, and mutants with a quantitative defect in type I collagen are indicated in orange. Blue bars indicate values that were statistically significantly altered for that mutant genotype, compared with its control as analyzed by the global test (see *SI Appendix*, Figs. S4–S19). Note the large variability in the effect of each mutation on the different parameters.

Given the joint involvement in human patients with a complete loss of α2(I) (6), we explored the presence of similar defects in *col1a2*$^{-/-}$ mutant fish. Histological analysis of the intervertebral ligament (IVL) showed a normal elastin layer, but reduced notochord sheath layer and a complete loss of type I collagen fibrous ligament, causing local distortion and dislocation of the IVL and intervertebral space in some parts of the vertebral column (Fig. 6D), which most likely underlies the kyphosis identified in this mutant and resembling the joint dislocations seen in human patients (6, 30, 31). The skin of *col1a2*$^{-/-}$ mutant fish was also more fragile and easily damaged, compared with the skin of wild-type control fish. Histological analysis of adult skin showed that the dermis, which is composed of two collagen fibril layers in zebrafish, is half the thickness in mutant fish compared with dermis of wild-type siblings (Fig. 6B). Biomechanical load-to-failure strength of soft connective tissues was analyzed by determining the ultimate tensile strength of tissue specimens from five *col1a2*$^{-/-}$ mutant and five control fish (Fig. 6C). Tissues lacking α2(I) ruptured at a significantly lower peak load (0.027 ± 0.0079 N), compared with tissue samples from wild-type siblings (0.081 ± 0.011 N, $P < 0.0001$), indicating significantly

diminished strength of soft connective tissue in *col1a2*$^{-/-}$ mutant fish. Histological sections of the adult zebrafish heart from *col1a2*$^{-/-}$ mutants showed normal morphological appearances of the cardiac valves and *col1a2*$^{-/-}$ larvae displayed normal cardiac function and blood flow (*SI Appendix*, Fig. S10).

**Genotype/Phenotype Relations in Mutants with Impaired Quality of Type I Collagen.** We next studied the skeleton of a set of mutants carrying a point mutation in either of the type I collagen-encoding genes, leading to impaired type I collagen quality (Fig. 1, Table 1, and *SI Appendix*, Figs. S11–S17). In human patients these types of mutations lead to OI types II–IV, which have moderate to severe or even lethal phenotypes with short stature, bone deformities, and hypermineralized bone (32, 33).

The *col1a2*$^{dmh15/+}$ mutant represents the most detrimental phenotype of all analyzed mutants (Fig. 1 and *SI Appendix*, Fig. S16), with heavily distorted, misshapen, and overmineralized axial and cranial skeletons. This is in concordance with human data because Gly substitutions in the homologous region of α2(I) are associated with lethal OI in human patients due to the presence of severe skeletal malformations early in fetal
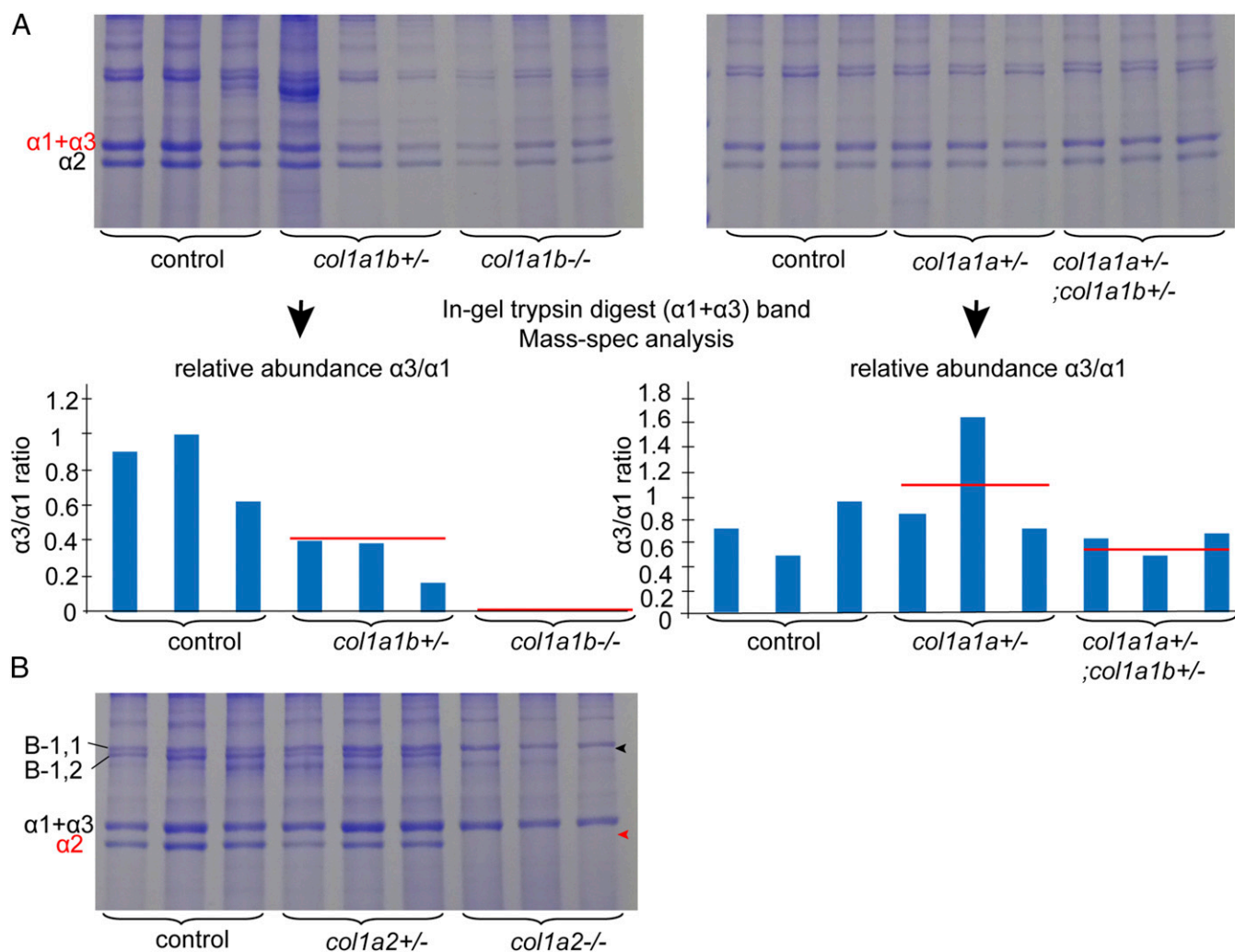
**Fig. 3.** SDS/PAGE and mass-spectrometry analysis of bone collagen from adult spine of *col1a1a, col1a1b,* and *col1a2* mutant fish with a quantitative type I collagen defect. (*A*) SDS/PAGE analysis of bone collagen extracted from individual adult spines of control fish, *col1a1b*^{+/−}, *col1a1b*^{−/−}, *col1a1a*^{+/−}, and *col1a1a*^{+/−}; *col1a1b*^{+/−} mutant fish. For each genotype, three biological replicates were taken into account. Following SDS/PAGE separation, an in-gel trypsin digest of the α1 (I) + α3(I) bands of each sample was performed and mass-spectrometry analysis was used to determine the relative amount of α1(I) and α3(I) in each sample. The expected α3(I)/α1(I) ratios (red lines in diagram) were approximated in samples from individual mutants (blue bars), illustrating that the reported nonsense mutations in *col1a1a* and *col1a1b* result in loss of the α1(I) chain and the α3(I) chain, respectively. Accordingly, in *col1a1b*^{−/−} mutants, no tryptic peptides of α3(I) could be detected, confirming decay of mutant *col1a1b* mRNA transcripts. (*B*) SDS/PAGE analysis of bone collagen extracted from individual adult spines of *col1a2*^{+/−} and *col1a2*^{−/−} mutant fish and control siblings. For each genotype, three biological replicates were taken into account. *Col1a2*^{−/−} mutant fish show a complete absence of *col1a2* encoded α2(I) (red arrowhead). Note also the absence of the β1,2 dimers (black arrowhead) in *col1a2*^{−/−} mutant fish.

development, in addition to other extraskeletal anomalies (Fig. 7) (34). The *col1a1a*[chi/+] mutant, reported earlier (21, 35), carries the same mutation that was identified in a human patient with severe and heavily deforming OI type III (34), and also displays a moderate to severe phenotype with skeletal malformation, including shorter vertebral bodies, kyphoscoliosis, and evidence of fractures (Fig. 1, Table 2, and *SI Appendix*, Fig. S13). The alleles *dmh13, dmh14,* and *dmh29* all cluster in the major ligand binding region 3 of type I collagen (Fig. 7), and while this region represents a hotspot for ligand interactions, mutations in this region are associated with variable phenotypic outcomes, ranging from moderate OI type IV to perinatal lethality (OI type II) (3, 34). This variability of phenotypic severity was also observed upon comparing the three different zebrafish mutants, with *col1a1b*[dmh29/+] fish displaying the most severe skeletal phenotype with kyphoscoliosis and shorter, thicker, and overmineralized vertebral bodies and frequent rib fractures (Fig. 1, Table 2, and *SI Appendix*, Figs. S14, S15, and S17). The *col1a1a med* allele, reported earlier by Asharani

et al. (20), was shown to have no effect in heterozygous state but caused pronounced effects on TMD, volume, and thickness of the vertebral bodies when present in homozygous state (*SI Appendix*, Figs. S11 and S12). However, as no comparable mutations have been identified in human patients, this *col1a1a*[med/med] mutant is likely less relevant for human OI.

To detect the presence of collagen overmodification, which is typically caused by collagen I glycine substitutions in human OI patients, collagen from adult bone was extracted by heat denaturation and subjected to SDS/PAGE. While migration of the α-chains was not affected in bone from *col1a2*[dmh15/+], *col1a1b*[dmh29/+], and *col1a1a*[med/med] mutants, retarded α-chain mobility, indicating collagen overmodification, was observed for *col1a1a*[chi/+], *col1a1a*[dmh13/+], and *col1a1a*[dmh14/+] mutants (Fig. 8).

## Discussion

In this work, we present a skeletal phenomic analysis of a set of zebrafish with mutations in type I collagen that model different
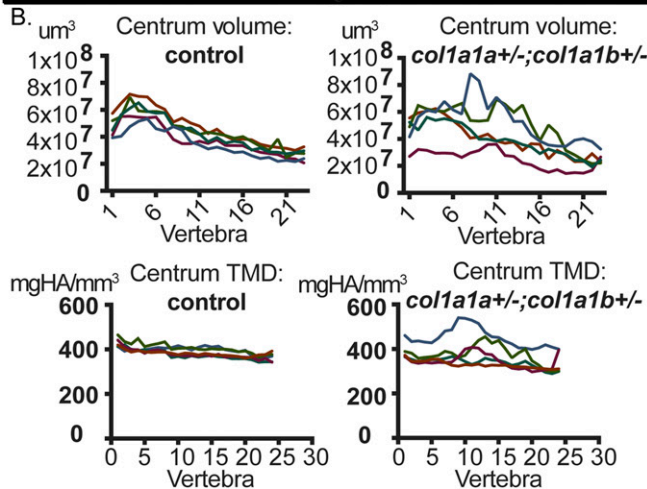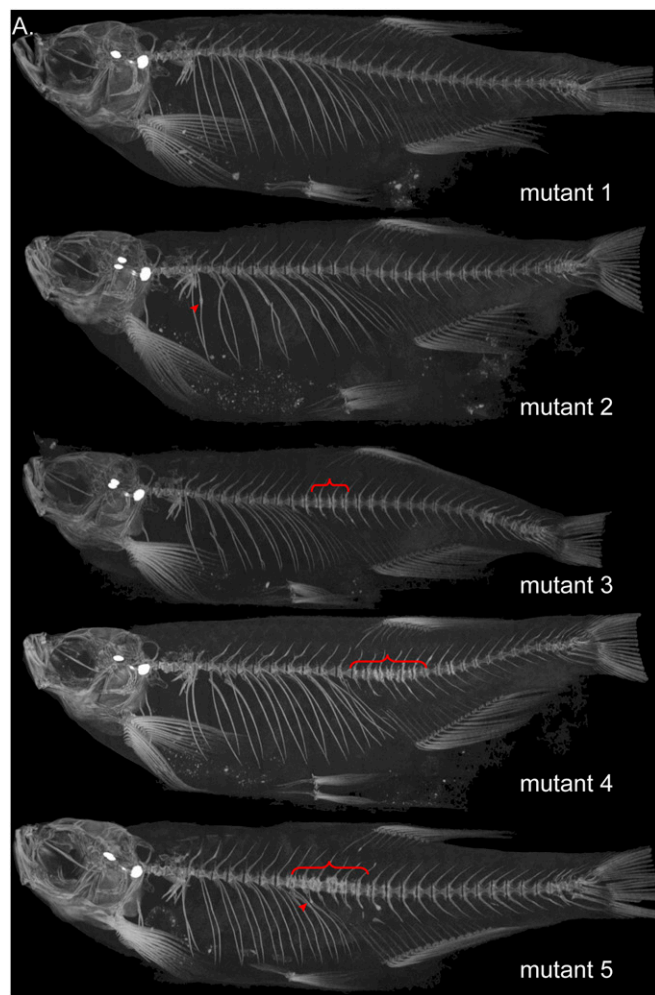
**Fig. 4.** col1a1a^{+/−};col1a1b^{+/−} mutant fish exhibit intragroup variability in phenotypic expressivity. (A) Different col1a1a^{+/−};col1a1b^{+/−} mutant siblings were analyzed using μCT scanning at 5 mo of age (mutant 1 to mutant 5). Upon comparison of the different mutant siblings, both incomplete penetrance and a variable expressivity of features indicative of compromised bone quality was observed, which include fractures (arrowheads) and local compressions in the vertebral column causing a distorted shape of the vertebral bodies (brackets). (B) Intragroup variability for col1a1a^{+/−};col1a1b^{+/−} mutant fish is demonstrated for volume and TMD of the vertebral centra, with values in the mutant group showing a much larger spread than compared with the control group. The different colors in one graph represent different individual fish of the same group (mutant siblings or control siblings).
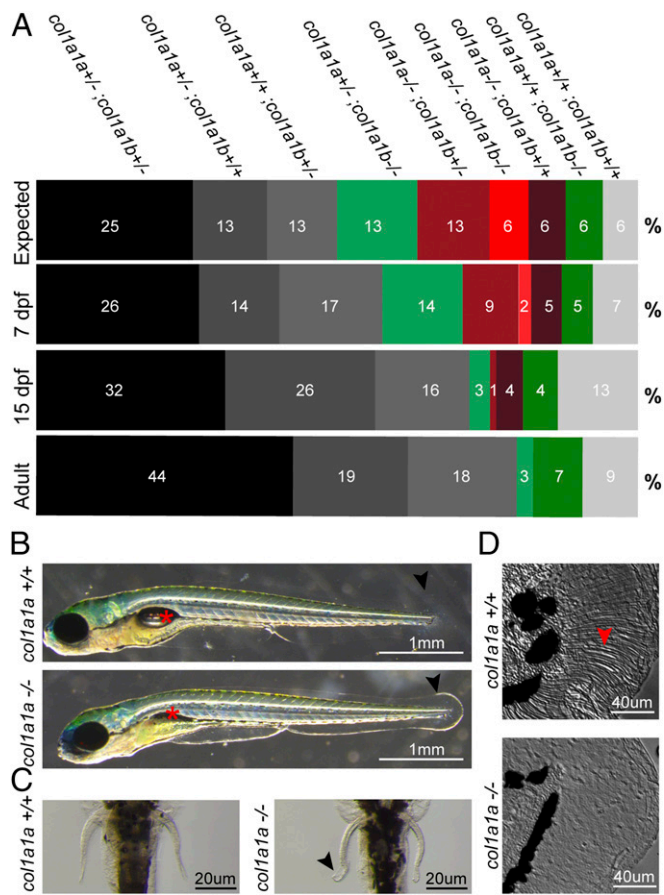


**Fig. 5.** In-depth analysis of mutants with partial or complete loss of col1a1a and/or col1a1b. (A) Segregation analysis of the different mutant genotypes generated from an in-cross of col1a1a^{+/−};col1a1b^{+/−} double-heterozygous mutant fish. Progeny were genotyped at three different time points (100 fish per time point): 7 dpf, 15 dpf, and adult stage (3 mo). The relative abundance of each genotype is given for each time point as a percentage. "Expected" indicates the theoretical abundance of each genotype, following Mendelian segregation. All combinations with a complete loss of col1a1a (col1a1a^{−/−}, indicated in red shades), are less viable and completely lost when progeny reached adulthood. Genotypes that contain a complete loss of col1a1b (col1a1b^{−/−}, indicated in green shades) are still present at adult stage. Black indicates the parental genotype, white indicates wild-type fish, and gray represents the other remaining genotypes. (B) Phenotype of col1a1a^{−/−} mutant larvae at 7 dpf, compared with wild-type siblings. Col1a1a^{−/−} mutant larvae present with a noninflated swimbladder (asterisk) and a ruffled finfold (arrowhead). (C) Ventral view and detail of the pectoral fins showing frilly distal margins (arrowhead) in the pectoral fins of col1a1a^{−/−} mutant larvae at 7 dpf. (D) Detail of the col1a1a^{−/−} mutant larvae finfold at 7 dpf, showing an absence of fin actinotrichia fibers, which can be clearly observed in the finfold of wild-type siblings (arrow).

type I collagenopathies, including the classic types of OI and a specific subtype of EDS. By systematically analyzing the skeletal phenotypes in this set of mutants, we illustrate the high ability of zebrafish mutants to reproduce the genetic and phenotypic features of type I collagenopathies.

OI in human patients is characterized by bone fragility, leading to a higher susceptibility to fractures, and in addition, misshapen bones and skeletal malformation can be observed (7). The presence of these disease features and the extent to which they manifest is largely associated with the specific subtype of OI (7). As such, quantitative defects in type I collagen, underlying OI type I, tend to cause mild skeletal defects in human patients with an increased susceptibility to fractures but minimal bone deformity. Zebrafish mutants with similar quantitative type I collagen
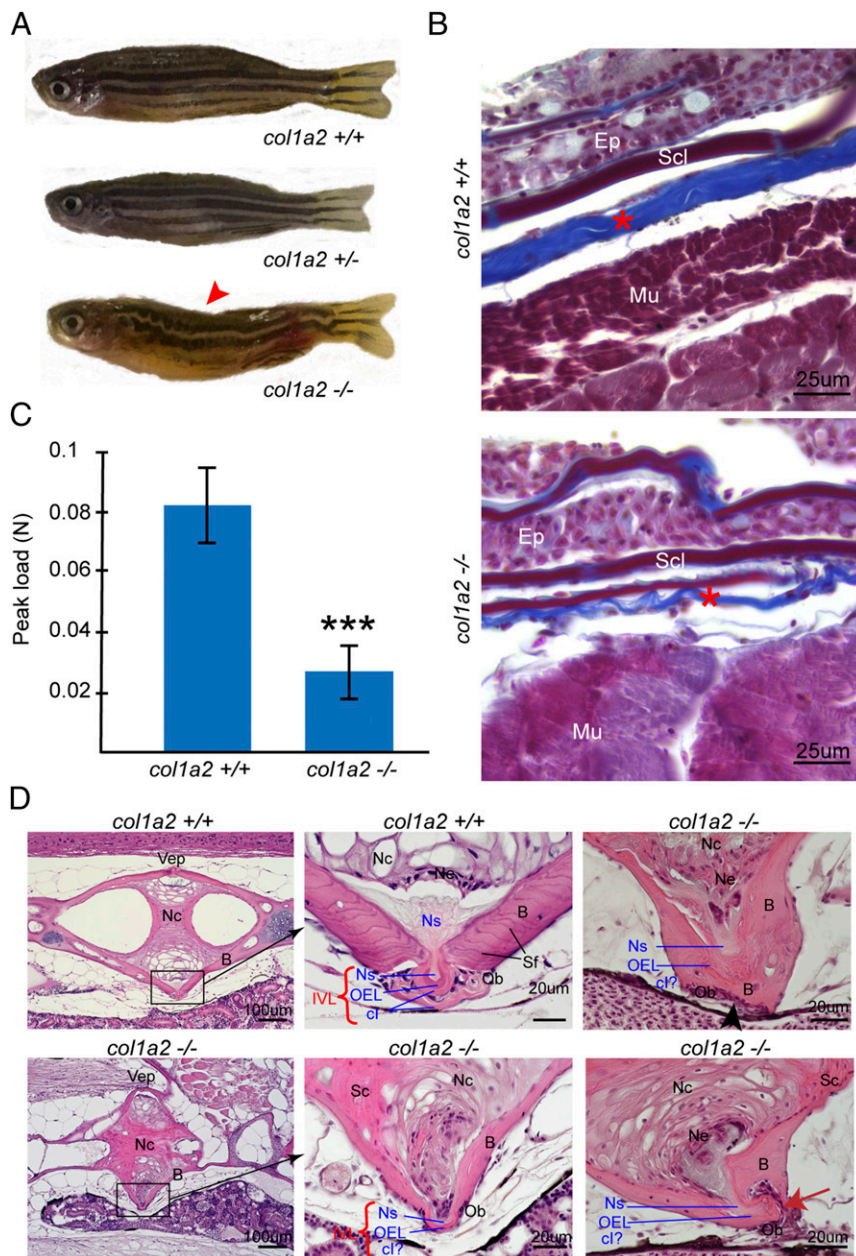
**Fig. 6.** In-depth analysis of col1a2$^{+/-}$ and col1a2$^{-/-}$ mutant fish. (*A*) Visual phenotype of col1a2 mutant and wild-type siblings. Both col1a2$^{+/+}$ control, and col1a2$^{+/-}$ mutant fish display a normal morphology, while col1a2$^{-/-}$ mutant are dysmorphic and display kyphosis (arrowhead). The typical stripe pattern in the skin is disturbed in col1a2$^{-/-}$ mutant fish, but normal in col1a2$^{+/+}$ controls and col1a2$^{+/-}$ mutant fish. (*B*) Masson's Trichrome staining of histological sections of the skin of an adult col1a2$^{-/-}$ mutant fish and a col1a2$^{+/+}$ control sibling. Note the much thinner dermis (asterisk), composed of layers of collagen fibrils (stained blue) in col1a2$^{-/-}$ mutant fish compared with col1a2$^{+/+}$ controls. (*C*) Average maximum tensile strength, measured by biomechanical testing of skin flaps dissected from five adult col1a2$^{-/-}$ mutant fish and five col1a2$^{+/+}$ control fish, illustrating strongly decreased strength of soft connective tissues in mutant fish ($P < 0.0001$). (*D*) Histological analysis of the vertebral column of adult fish, sagittal sections stained with H&E. Shown at the *Left* are two adjoining vertebral body endplates (Vep, i.e., the region where two adjacent vertebral bodies meet and are connected by the IVL) in a col1a2$^{+/+}$ control and a col1a2$^{-/-}$ mutant adult fish. The black rectangles indicate the region which is shown at a higher magnification in the image next to it on the *Right*, depicting the IVL in detail. In control fish, the IVL is typically composed of three distinct layers or tissues: the notochord sheet (Ns, mainly type II collagen), the outer elastin layer (OEL), and a layer of type I collagen fiber bundles (cI). In the col1a2$^{-/-}$ mutants, IVL composition is abnormal: the OEL was still present, the Ns layer could be observed but was extremely reduced, but no layer of type I collagen fibers (cI) could be observed. Col1a2$^{-/-}$ mutant bone (B) in the vertebral bodies near the Vep showed a loss of typical Sharpey fibers (Sf), while the notochord cells (Nc) displayed a loss of vacuoles, in addition to sclerosis (Sc). As shown in the two rightmost pictures, we observed fusions of adjacent vertebral bodies (black arrowhead) and dislocation of the IVL and Vep (red arrow) in some of the vertebrae, likely resulting in kyphosis seen in col1a2$^{-/-}$ mutant fish. Other abbreviations: Ep, epidermis; Mu, muscle fibers; Ob, osteoblasts; Scl, Scale.

defects (col1a1a$^{+/-}$;col1a1b$^{+/-}$ mutants) also presented with increased fracture risk, apparent from the presence of spontaneous fractures in the ribs, while skeletal deformities were minimal with only localized and mild compressions of the vertebral column in some of the mutant fish. Conversely, qualitative type I collagen defects in zebrafish evoked a more pronounced effect on the skeleton, with frequent fractures, kyphoscoliosis and malformation of the vertebral bodies, and misshapen ribs and fin bones. These phenotypes correspond to the moderately severe, progressive deforming or lethal clinical phenotypes of OI types II–IV. Importantly, the more severely affected mutants of this group (dmh15 and dmh29) also displayed overmineralization in the vertebral column, a feature often seen in human OI, and especially associated with the more severe cases in human patients (32, 33). Additionally, biochemical analysis argued for type I collagen overmodification, one of the typical features in human OI, in some of the mutants with a qualitative defect. Moreover, the variability of the excessive posttranslational modification

throughout this set of mutants corresponds to the situation in human patients with OI types II–IV, where variable collagen overmodification has been related to the position of the mutation in the type I collagen helix (34, 36). Overall, the genotype–phenotype analysis we performed shows the validity of the included zebrafish mutants as models for different forms of human OI.

A hallmark feature of OI in humans is the large clinical spectrum of phenotypes, with disease presentation that can differ from very mild to perinatal lethal, even with the same causative mutation. The underlying molecular basis of this variability remains largely not understood. The zebrafish mutants described here similarly show significant variation in their expressivity. Intragenotype variability is illustrated in col1a1a$^{+/-}$;col1a1b$^{+/-}$ mutant siblings, as some show fractured ribs or vertebral compressions, while others do not. In addition, there is a large variability in vertebral morphology and mineralization in mutant siblings, in contrast to control siblings. A likely explanation for
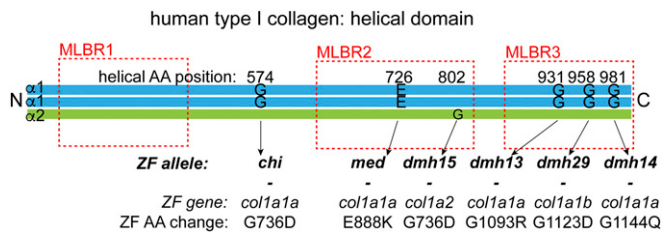
**Fig. 7.** Zebrafish alleles representing amino acid substitutions in type I collagen mapped on the helical domain of human type I collagen. The α1 and α2 chains of the human type I collagen are schematically depicted with the three major ligand binding regions (MLBR), indicated with red stripped lines (34). The homologous positions to the zebrafish (ZF) alleles (as determined by Clustal W analysis), representing mutations that cause an amino acid (AA) substitution, are indicated with arrows. The numbering of the zebrafish alleles indicates the total protein position of the residue.

the intragenotype phenotypic variability in zebrafish mutants is the highly polymorphic nature of its genome, which closely resembles human genetic variability. This makes them particularly useful to unveil genetic determinants that can be used to map potential regulation of phenotypic variability in humans. This is less obvious in mouse models, where mostly inbred strains are used for disease modeling (37, 38).

In zebrafish, type I collagen has been shown to have a different composition than in mammals, with two orthologs of the human *COL1A1* gene, namely *col1a1a* and *col1a1b*, encoding the α1- and α3-chain, respectively. Some insights in these differences have already been addressed previously (19), and by studying different knockout mutants for the type I collagen genes we further extend this knowledge. Heterozygous loss of either α1(I) or α3(I) did not induce any skeletal abnormalities, while reduced levels of both α1(I) and α3(I) (*col1a1a$^{+/-}$;col1a1b$^{+/-}$* mutants) causes a mild skeletal phenotype with increased bone fragility, arguing for interchangeability and functional redundancy between α1(I) and the homologous α3(I). Complete loss of the α1(I) chain causes lethality after 7 dpf, while loss of α3(I) only shows increased early lethality if the amount of α1(I) is also diminished. This suggests a gene/protein dosage effect, where α1(I) is more abundant than α3(I), as hypothesized in our previous work (19). The functional similarity between α1(I) and α3(I) is further illustrated by the fact that glycine substitutions in both genes can cause severe skeletal phenotypes, arguing for a dominant-negative effect on type I bone collagen and thus incorporation of a substantial amount of both α1(I) and α3(I) into the type I collagen triple helix. However, to obtain a full understanding of zebrafish type I collagen, the exact trimer stoichiometry in different tissues, and the abundance of each possible trimer composition should be examined, which is technically challenging due to the small specimen size of zebrafish compared with the large amount of input material needed for standard biochemical analysis techniques.

In humans, haploinsufficiency for the α2(I)-chain does not cause a clinically significant phenotype, while complete loss of α2(I) leads to the very rare cardiac valvular subtype of the EDS, associated with soft connective tissue defects, including skin and joint manifestations and propensity to cardiac valvular defects, and relatively mild skeletal manifestations (6). These trends were mostly recapitulated in zebrafish, as *col1a2$^{+/-}$* mutants are asymptomatic, whereas *col1a2$^{-/-}$* mutants display an EDS-like phenotype with different connective tissue defects; μCT-scanning showed local vertebral abnormalities, including kyphosis, and a mild reduction of bone thickness and mineralization. Histological analysis demonstrated dislocation and distortion of the fibrous connections between some of the vertebral bodies, caused by degeneration of the layers composing the connecting intervertebral ligament. Most

likely the latter defect is the cause of the kyphosis seen in these mutants, with the location of the kyphosis being the area bearing the highest mechanical force in the fish vertebral column (34). Similar to these observations, patients with the same molecular defect display joint dislocations but no severe skeletal involvement (6). Interestingly, *col1a2$^{-/-}$* mutant fish showed fragile skin upon handling and histological analysis demonstrated a much thinner dermis in the skin of mutant fish compared with wild-type siblings. Consistent with these findings, bio-mechanical testing argued for a strongly reduced strength of soft connective tissues in *col1a2$^{-/-}$* mutant fish. This relates to other clinical hallmark features of the skin in human cardiac valvular EDS patients (6). Preliminary experiments in *col1a2$^{-/-}$* mutant fish could not provide any proof of defects in cardiac morphology or functioning. However, more extensive analyses are needed to further explore a possible impaired cardiac function in a follow-up study, focusing on an in-depth characterization of this mutant, which was beyond the scope of the study presented here.

Taken together, we have analyzed a large set of zebrafish models with mutations in type I collagen that represent different type I collagenopathies, including the classic types of OI and a specific subtype of EDS, and illustrate the high phenotypic and genetic similarity of these zebrafish mutants with human type I collagenopathies. We further report a zebrafish model resembling the human EDS, which harbors a number of characteristic defects in the soft connective tissues. Our study surpasses the analysis at the single-mutant model level but illustrates the occurrence of relevant phenotypic patterns and characteristics across a large set of genetically distinct zebrafish models. These results, taken together with the feasibility of zebrafish for easily accommodating large genetic and phenotypic screens, argue for zebrafish as a promising tool in future research aiming to dissect the underlying basis of phenotypical variability in human type I collagenopathies, such as OI. Furthermore, we provide more insight into the biology of zebrafish type I collagen and its consequences, which are relevant in the study of any human type I collagen related disease by using zebrafish as a model.

## Material and Methods

**Animals.** The *col1a1a$^{sa1748}$*, *col1a1b$^{sa12931}$*, *col1a2$^{sa17981}$*, *bmp1a$^{sa2416}$*, and *plod2$^{sa1768}$* mutant zebrafish were generated by the zebrafish mutation project and together with wild-type AB fish obtained from the zebrafish international resource center (ZIRC, zebrafish.org/home/guide.php) or the European Zebrafish Resource center [EZRC, www.ezrc.kit.edu)] (39). The *col1a1a$^{chi}$* were previously described (21) and the *col1a1a$^{med}$* mutant fish were
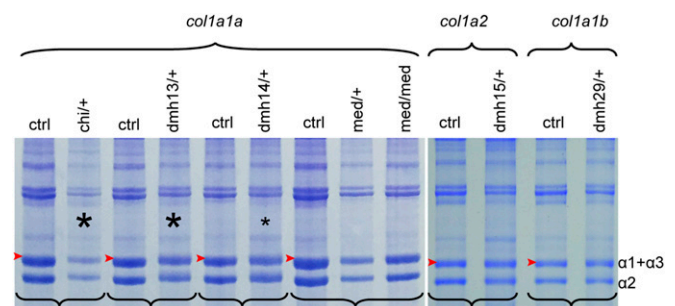


**Fig. 8.** SDS/PAGE of collagen extracted from the bone of adult mutants with qualitative type I collagen defects. SDS/PAGE analysis of acid soluble collagen extracts from different mutant genotypes carrying amino acid substitutions in α1(I), α2(I), or α3(I), and from matching wild-type control (ctrl) siblings (sibling pairs indicated by brackets, in each pair the height of the α1 + α3 band in the WT control is indicated by the red arrow) indicate that α-band migration is markedly slower for *col1a1a$^{chi/+}$* and *col1a1a$^{dmh13/+}$* mutants, and only slightly decreased in *col1a1a$^{dmh14/+}$* mutants (lanes indicated by asterisks), compared with the corresponding control. No apparent signs of collagen overmodification could be detected for the other mutant genotypes.

purchased from the EZRC. The *col1a1a*[dmh13], *col1a1a*[dmh14], *col1a1b*[dmh29], and *col1a2*[dmh15] mutant fish were generated in a forward genetics screen (40). Fish husbandry was performed as previously described (22). Studies were done in agreement with EU Directive 2010/63/EU for animals, permit Number: ECD 17/68. All efforts were made to minimize pain and discomfort.

**µCT Scanning and Analysis.** µCT-based phenotyping and quantification of adult zebrafish was performed as previously described (25). For each genotype five mutants and five control fish were analyzed.

**Collagen Analysis.** Collagen analysis of adult zebrafish bone was performed as described previously (22). To determine a relative mount of α1(I)- and α3(I)-chains, a unique tryptic peptide for each α1(1) and for α3(1) was selected and the relative amount of the corresponding peak manually measured on the full scan by determining peak height. For all mutant genotypes an expected ratio of α3(I)/α1(I) was calculated based on the mean relative α3(I)/α1(I) ratio observed in control samples and based on the assumption of absence of α3(I) and α1(I) in the case of knockout of *col1a1b* and *col1a1a*, respectively.

**Histological Analysis.** Histological analysis of zebrafish tissues was performed as described in Gistelinck et al. (22).

**Bio-Mechanical Testing.** Soft connective tissue sections were isolated from 5 mo old *col1a2*^{−/−} mutant fish ($n = 5$) and wild-type control siblings ($n = 5$) by decapitation and dissecting away the spine from each specimen. These tissue specimens were kept in PBS for a maximum period of 8 h. Uniaxial tensile tests were performed at room temperature using an Instron 5942 electromechanical test system (Instron), as previously described (41).

Detailed information regarding the procedures used is provided in *SI Appendix, Supplementary Material and Methods*.

1. van der Rest M, Garrone R (1991) Collagen family of proteins. *FASEB J* 5:2814–2823.
2. Jobling R, et al. (2014) The collagenopathies: Review of clinical phenotypes and molecular correlations. *Curr Rheumatol Rep* 16:394.
3. Marini JC, et al. (2007) Consortium for osteogenesis imperfecta mutations in the helical domain of type I collagen: Regions rich in lethal mutations align with collagen binding sites for integrins and proteoglycans. *Hum Mutat* 28:209–221.
4. Sillence DO, Senn A, Danks DM (1979) Genetic heterogeneity in osteogenesis imperfecta. *J Med Genet* 16:101–116.
5. Forlino A, Marini JC (2015) Osteogenesis imperfecta. *Lancet*.
6. Malfait F, et al. (2006) Total absence of the alpha2(I) chain of collagen type I causes a rare form of Ehlers-Danlos syndrome with hypermobility and propensity to cardiac valvular problems. *J Med Genet* 43:e36.
7. Marom R, Lee YC, Grafe I, Lee B (2016) Pharmacological and biological therapeutic strategies for osteogenesis imperfecta. *Am J Med Genet C Semin Med Genet* 172:367–383.
8. Ben Amor IM, Glorieux FH, Rauch F (2011) Genotype-phenotype correlations in autosomal dominant osteogenesis imperfecta. *J Osteoporos* 2011:540178.
9. Rauch F, Lalic L, Roughley P, Glorieux FH (2010) Genotype-phenotype correlations in nonlethal osteogenesis imperfecta caused by mutations in the helical domain of collagen type I. *Eur J Hum Genet* 18:642–647.
10. Pollitt RC, et al. (2016) Phenotypic variability in patients with osteogenesis imperfecta caused by BMP1 mutations. *Am J Med Genet A* 170:3150–3156.
11. Rauch F, et al. (2013) Osteogenesis imperfecta type V: Marked phenotypic variability despite the presence of the IFITM5 c.-14C>T mutation in all patients. *J Med Genet* 50:21–24.
12. Valadares ER, Carneiro TB, Santos PM, Oliveira AC, Zabel B (2014) What is new in genetics and osteogenesis imperfecta classification? *J Pediatr (Rio J)* 90:536–541.
13. Laize V (2014) Fish: A suitable system to model human bone disorders and discover drugs with osteogenic or osteotoxic activities. *Drug Discovery Today Dis Models* 13:29–37.
14. Witten PE, Harris MP, Huysseune A, Winkler C (2017) Small teleost fish provide new insights into human skeletal diseases. *Methods Cell Biol* 138:321–346.
15. Kamoun-Goldrat AS, Le Merrer MF (2007) Animal models of osteogenesis imperfecta and related syndromes. *J Bone Miner Metab* 25:211–218.
16. Harris MP, Henke K, Hawkins MB, Witten PE (2014) Fish is fish: The use of experimental model species to reveal causes of skeletal diversity in evolution and disease. *J Appl Ichthyology* 30:616–629.
17. Apschner A, Schulte-Merker S, Witten PE (2011) Not all bones are created equal—Using zebrafish and other teleost species in osteogenesis research. *Methods Cell Biol* 105:239–255.
18. Mackay EW, Apschner A, Schulte-Merker S (2013) A bone to pick with zebrafish. *Bonekey Rep* 2:445.
19. Gistelinck C, et al. (2016) Zebrafish collagen type I: Molecular and biochemical characterization of the major structural protein in bone and skin. *Sci Rep* 6:21540.
20. Asharani PV, et al. (2012) Attenuated BMP1 function compromises osteogenesis, leading to bone fragility in humans and zebrafish. *Am J Hum Genet* 90:661–674.
21. Fisher S, Jagadeeswaran P, Halpern ME (2003) Radiographic analysis of zebrafish skeletal defects. *Dev Biol* 264:64–76.
22. Gistelinck C, et al. (2016) Loss of type I collagen telopeptide lysyl hydroxylation causes musculoskeletal abnormalities in a zebrafish model of Bruck syndrome. *J Bone Miner Res* 31:1930–1942.
23. Symoens S, et al. (2015) Genetic defects in TAPT1 disrupt ciliogenesis and cause a complex lethal osteochondrodysplasia. *Am J Hum Genet* 97:521–534.
24. Charles JF, et al. (2017) Utility of quantitative micro-computed tomographic analysis in zebrafish to define gene function during skeletogenesis. *Bone* 101:162–171.
25. Hur M, et al. (2017) MicroCT-based phenomics in the zebrafish skeleton reveals virtues of deep phenotyping in a distributed organ system. *eLife* 6:e26014.
26. Durán I, Marí-Beffa M, Santamaría JA, Becerra J, Santos-Ruiz L (2011) Actinotrichia collagens and their role in fin formation. *Dev Biol* 354:160–172.
27. Duran I, et al. (2015) Collagen duplicate genes of bone and cartilage participate during regeneration of zebrafish fin skeleton. *Gene Expr Patterns* 19:60–69.
28. van Eeden FJ, et al. (1996) Genetic analysis of fin formation in the zebrafish, Danio rerio. *Development* 123:255–262.
29. Nicholls AC, Valler D, Wallis S, Pope FM (2001) Homozygosity for a splice site mutation of the COL1A2 gene yields a non-functional pro(alpha)2(I) chain and an EDS/OI clinical phenotype. *J Med Genet* 38:132–136.
30. Bensimon-Brito A, Cardeira J, Cancela ML, Huysseune A, Witten PE (2012) Distinct patterns of notochord mineralization in zebrafish coincide with the localization of Osteocalcin isoform 1 during early vertebral centra formation. *BMC Dev Biol* 12:28.
31. Kvellestad A, Høie S, Thorud K, Tørud B, Lyngøy A (2000) Platyspondyly and shortness of vertebral column in farmed Atlantic salmon Salmo salar in Norway—Description and interpretation of pathologic changes. *Dis Aquat Organ* 39:97–108.
32. Bishop N (2016) Bone material properties in osteogenesis imperfecta. *J Bone Miner Res* 31:699–708.
33. Boyde A, Travers R, Glorieux FH, Jones SJ (1999) The mineralization density of iliac crest bone from children with osteogenesis imperfecta. *Calcif Tissue Int* 64:185–190.
34. Sweeney SM, et al. (2008) Candidate cell and matrix interaction domains on the collagen fibril, the predominant protein of vertebrates. *J Biol Chem* 283:21187–21197.
35. Gioia R, et al. (2017) The chaperone activity of 4PBA ameliorates the skeletal phenotype of Chihuahua, a zebrafish model for dominant osteogenesis imperfecta. *Hum Mol Genet* 26:2897–2911.
36. Cabral WA, Milgrom S, Letocha AD, Moriarty E, Marini JC (2006) Biochemical screening of type I collagen in osteogenesis imperfecta: Detection of glycine substitutions in the amino end of the alpha chains requires supplementation by molecular analysis. *J Med Genet* 43:685–690.
37. Guryev V, et al. (2006) Genetic variation in the zebrafish. *Genome Res* 16:491–497.
38. Sigmund CD (2000) Viewpoint: Are studies in genetically altered mice out of control? *Arterioscler Thromb Vasc Biol* 20:1425–1429.
39. Kettleborough RN, et al. (2013) A systematic genome-wide analysis of zebrafish protein-coding gene function. *Nature* 496:494–497.
40. Henke K, et al. (2017) Genetic screen for postembryonic development in the zebrafish (*Danio rerio*): Dominant mutations affecting adult form. *Genetics* 207:609–623.
41. Christensen H, Andreassen TT, Oxlund H (1992) Age-related alterations in the strength and collagen content of left colon in rats. *Int J Colorectal Dis* 7:85–88.